

# Effects of cholesterol on thermal stability of discoidal high density lipoproteins<sup>S</sup>

Shobini Jayaraman,<sup>1</sup> Sangeeta Benjwal, Donald L. Gantz, and Olga Gursky

Department of Physiology and Biophysics, Boston University School of Medicine, Boston, MA 02118

**Abstract** Reverse cholesterol transport in plasma involves variations in HDL cholesterol concentration. To understand physicochemical and functional implications of such variations, we analyzed stability of reconstituted HDL containing human apolipoproteins (apoA-I, apoA-II, or apoC-I), phosphatidylcholines varying in chain length (12–18 carbons) and unsaturation (0 or 1), and 0–35 mol% cholesterol. Lipoprotein heat denaturation was monitored by circular dichroism for protein unfolding/dissociation and by light scattering for particle fusion. We found that cholesterol stabilizes relatively unstable complexes; for example, incorporation of 10–30 mol% cholesterol in apoC-I:dimyristoyl phosphatidylcholine complexes increased their kinetic stability by  $\delta\Delta G^* \equiv 1$  kcal/mol. In more stable complexes containing larger proteins and/or longer-chain lipids, incorporation of 10% cholesterol did not significantly alter the disk stability; however, 15% or more cholesterol destabilized the apoA-I-containing complexes and led to vesicle formation. Thus, cholesterol tends to stabilize less stable lipoproteins, apparently by enhancing favorable packing interactions, but in more stable lipoproteins, where such interactions are already highly optimized, the stabilizing effect of cholesterol decreases and, eventually, becomes destabilizing. These results help uncouple the functional roles of particle stability and chain fluidity and suggest that structural disorder in HDL surface, rather than chain fluidity, is an important physicochemical determinant of HDL function.—Jayaraman, S., S. Benjwal, D. L. Gantz, and O. Gursky. **Effects of cholesterol on thermal stability of discoidal high density lipoproteins.** *J. Lipid Res.* 2010. 51: 324–333.

**Supplementary key words** kinetic stability • protein unfolding rate • lipoprotein fusion • acyl chain fluidity • reverse cholesterol transport

Cholesterol is an essential constituent of eukaryotic cells. It is an important signaling molecule and a metabolic precursor of bile acids, steroid hormones, and vitamin D; in addition, it imparts unique physical properties to cell membranes, which may be crucial for biological

function. Cholesterol stabilizes the liquid-ordered ( $L_o$ ) phase in fluid bilayers, reduces bilayer fluidity and permeability, increases the bilayer thickness, organizes the membrane into microdomains or rafts, and modulates membrane fusion (Refs. 1–6 and references therein). Cholesterol concentration in the plasma membrane is tightly regulated by a balance between the endogenous synthesis, influx of exogenous cholesterol from LDL, and efflux of excess cholesterol to HDL (7). An imbalance among these processes may lead to major diseases, such as atherosclerosis.

The cardioprotective effects of HDL and their major protein, apolipoprotein A-I (apoA-I; 28 kDa), are attributed mainly to their role in reverse cholesterol transport (RCT), which is the sole pathway of cholesterol removal from the body (for recent review, see Ref. 8). In RCT, HDL and their precursors stimulate efflux of free (unesterified) cholesterol from the peripheral tissue cells, including macrophages, facilitate its esterification by LCAT, and transport cholesterol esters to the liver for excretion via bile or to steroidogenic organs for hormone synthesis. At an early step of RCT, interactions of lipid-poor apoA-I with the plasma membrane, which are mediated by the ATP-binding cassette transporter A1, lead to the formation of nascent discoidal HDL (9, 10). These small particles (diameter of  $\sim 7$ –9 nm) comprise a cholesterol-containing phospholipid bilayer and two or more copies of apoA-I and/or other exchangeable (water-soluble) apolipoproteins that are thought to adopt a belt-like  $\alpha$ -helical conformation around the particle perimeter, screening the acyl chains from the aqueous milieu (Refs. 11–13 and references therein). Nascent HDL, whose free cholesterol

Abbreviations: apo, apolipoprotein; CD, circular dichroism; Ch, unesterified cholesterol; DLPC, dilinoleyl phosphatidylcholine; DMPC, dimyristoyl phosphatidylcholine; DPPC, dipalmitoyl phosphatidylcholine; DSC, differential scanning calorimetry; EM, electron microscopy; PC, phosphatidylcholine; POPC, palmitoyl oleoyl phosphatidylcholine; RCT, reverse cholesterol transport; rHDL, reconstituted high-density lipoprotein; T-jump, temperature jump.

<sup>1</sup>To whom correspondence should be addressed.

e-mail: shobini@bu.edu

<sup>S</sup>The online version of this article (available at <http://www.jlr.org>) contains supplementary data.

This work was supported by the National Institutes of Health Grants GM-67260 and HL-26355. Its contents are solely the responsibility of the authors and do not necessarily represent the official views of the National Institutes of Health.

Manuscript received 3 August 2009 and in revised form 10 August 2009.

Published, JLR Papers in Press, August 10, 2009  
DOI 10.1194/jlr.M000117

concentration usually varies from about 4–10 mol% (14–16), acquire additional cholesterol by passive diffusion (limited by the nanomolar aqueous solubility of cholesterol) or by active efflux mediated by ATP-binding cassette G1 transporter (17) and form preferred substrates for LCAT. Cholesterol esters produced by LCAT are sequestered in the particle core, leading to HDL conversion from nascent discoidal to mature spheroidal particles. After further remodeling by LCAT and other lipophylic enzymes and lipid transporters (18), mature spherical HDL deliver their cargo of cholesterol esters via the receptor-mediated selective uptake of apolar lipids (reviewed in Refs. 8 and 19).

During RCT, cholesterol concentration in nascent HDL undergoes dynamic variations. To assess the effects of such variations on the particle stability, we use reconstituted HDL (rHDL) containing apolipoproteins, phosphatidylcholines (PCs), and variable amounts of free cholesterol (Ch). Such rHDL provides useful structural and functional models for nascent plasma HDL (20). Earlier studies of discoidal rHDL have shown that incorporation of cholesterol may alter the apolipoprotein conformation (20–23), increase the particle diameter (Refs. 24 and 25 and references therein), and increase the net negative charge on HDL (21). The latter probably results from the cholesterol-induced reduction in the depth of lipid surface penetration by the amphipathic apolipoprotein  $\alpha$ -helices (26, 27), which normalizes the pKs of several lysines located at the lipid surface (21). These and other cholesterol-induced structural changes, such as increased bilayer thickness, reduced area per PC head group and reduced chain fluidity in the physiologically relevant fluid phase, and preferential exclusion of cholesterol from the apolipoprotein-containing lipid boundary reported in numerous studies (Refs. 27–31 and references therein) are expected to affect HDL function and stability (21, 32). This work addresses the effects of free cholesterol on structural stability of nascent rHDL.

Earlier studies of the effects of variations in HDL surface lipid composition (such as PC acyl chain length and unsaturation, sphingomyelin content, etc.) have reported a direct correlation between acyl chain fluidity and function of discoidal rHDL in stimulating cell cholesterol efflux or activating LCAT (Refs. 31, 33–35, and references therein). This led to a widely accepted notion that increased chain fluidity in surface lipids is beneficial for HDL function in RCT. Paradoxically, this implies that cholesterol incorporation in HDL disks, which reduces chain fluidity in physiologically relevant liquid phase (34), will impede HDL function, a notion that is not supported by the existing data. In fact, increase in cholesterol content has no effect on the binding affinity of LCAT to rHDL and increases the maximal rate of catalysis by increasing substrate concentration (32). Similarly, other functional reactions, such as apoA-I-induced bilayer microsolvubilization resulting in rHDL disk formation, are not adversely affected by the sterol-induced reduction in chain fluidity (36); to the contrary, incorporation of 5% cholesterol reportedly accelerated solubilization of dimyristoyl PC

(DMPC) by apoA-I (36). Furthermore, the effects of cholesterol on the apoA-I binding to the PC bilayer have been attributed to the changes in the head group spacing rather than chain fluidity (24, 26). Taken together, these results challenge the direct causal link between acyl chain fluidity and HDL function in RCT.

Alternatively, HDL function may be facilitated by the localized surface disorder at the head group, but not necessarily acyl chain, level. In fact, transient openings in HDL surface may facilitate insertion of cholesterol, LCAT, and other plasma factors, which is necessary for HDL remodeling in RCT (37, 38). This notion is consistent with an inverse relation observed between the stability of HDL subclasses and their functions in RCT (37–39). For example, discoidal rHDL comprised of shorter-chain PCs have lower kinetic stability (i.e., undergo faster denaturation) and provide better acceptors of cell cholesterol and better activators of LCAT than their longer-chain physiologic counterparts (Ref. 37 and references therein). Similarly, mature plasma HDL differing in particle size, composition, and oxidation degree showed an inverse correlation between their kinetic stability and function: the lower the stability, the faster the metabolic remodeling of HDL, which is beneficial for cardioprotection (38, 39). Taken together, these studies suggest that reduction in global stability promotes local structural fluctuations in lipoprotein surface, which accelerate metabolic remodeling necessary for HDL function in RCT (38). Similarly, in many proteins and their complexes, reduction in global structural stability facilitates local structural fluctuations that are important for protein function (Ref. 38 and references therein).

Analysis of the effects of cholesterol on HDL stability may help to differentiate between these alternatives. Earlier stability studies of cholesterol-containing rHDL, which reported that incorporating more than two cholesterol molecules per particle destabilized rHDL, have been focused on complexes of apoA-I and palmitoyl-oleoyl PC (POPC) (32). This and many other HDL stability studies relied on end-point measurements after incubation with denaturant, an equilibrium thermodynamic approach whose application to irreversible lipoprotein denaturation is often inconclusive (Ref. 39 and references therein). Later, we showed that HDL stability is determined by free energy barriers that decelerate protein dissociation and lipoprotein fusion during denaturation and developed a novel kinetic approach for quantitative analysis of lipoprotein stability (40). In this approach, kinetic stability is defined as a height of the free energy barrier separating native (N) from the denatured (D) state,  $\Delta G^* = G^* - G_N$ , where  $G^*$  is free energy of the transition state; this contrasts with thermodynamic stability defined as  $\Delta G = G_D - G_N$ . In lipoprotein denaturation, high free energy of the transition state, and hence high  $\Delta G^*$ , arise from transient disruption of protein and lipid packing interactions and transient solvent exposure of apolar groups during apolipoprotein dissociation and lipoprotein fusion (40). The value of  $\Delta G^*$  is assessed from the comparison of the denaturation rates  $k$  measured in kinetic experiments, with the

rates  $K$  in the absence of the barrier,  $\Delta G^* = -RT \cdot \ln k/K$ . Thus, the higher is  $\Delta G^*$ , the lower is  $k$ , and the slower the denaturation.

Here, we use the kinetic approach to compare the stability of various rHDL containing different amounts of cholesterol. To do so, we use complexes of human apoA-I, apoA-II (the second-major HDL protein of 17 kDa), or apoC-I (6 kDa; the smallest exchangeable apolipoprotein that is a structural and functional prototype of larger proteins) (Ref. 40 and references therein) with fully saturated PC varying in chain length [dilinoleyl PC (DLPC; 12:0,12:0), DMPC (14:0,14:0), and dipalmitoyl PC (DPPC; 16:0,16:0)] or with monounsaturated POPC (16:0, 18:1). The results show that cholesterol stabilizes some of the less stable complexes, such as apoC-I:DMPC, but has no stabilizing effect on more stable disks, such as apoA-II or apoA-I-containing rHDL, and may even destabilize these complexes at 15 mol% and greater concentrations. Consequently, reduction in chain fluidity does not necessarily increase rHDL stability. This helps explain why reduction in fluidity upon cholesterol incorporation does not impair HDL function in RCT.

## MATERIALS AND METHODS

### Proteins and lipids

Lipids, including DLPC, DMPC, DPPC, POPC, and Ch, were 95%+ pure from Avanti Polar Lipids. Human apoA-I and apoA-II were isolated and purified from plasma HDL of healthy volunteer donors and refolded as described (41). The protein purity assessed by SDS-PAGE was 95%+. At the final stages of this project, we used recombinant apoA-I obtained by using a bacterial expression system (42) (kind gift of Dr. Michael Oda); the results of our structural and stability studies using plasma (Figs. 1–3) and recombinant apoA-I (data not shown) were in excellent agreement. Because of the limited amount of apoA-II available for this project, our studies were focused on the apoA-II-containing complexes that had discoidal morphology. Human apoC-I with unblocked termini was custom-synthesized and purified to 97%+ purity by solid state synthesis at 21st Century Biochemicals as described (40); the peptide identity and purity were confirmed by mass spectrometry and HPLC. All chemicals were highest purity analytical grade.

### Lipoprotein reconstitution and characterization

Discoidal complexes containing DLPC or DMPC (with or without cholesterol) were prepared by thin film evaporation (20). Briefly, multilamellar vesicles were prepared by dissolving the lipids (Ch:PC molar ratio from 0:100 to 30:70) in two parts chloroform and one part methanol; organic solvent was evaporated under nitrogen stream overnight, and the samples were dried under vacuum overnight at 4°C to ensure complete solvent removal. Lipid films were dispersed by vortexing in 10 mM sodium phosphate buffer, pH 7.5 (the standard buffer used throughout this study). The protein was added to the lipid suspension (PC to protein molar ratio was 165:1 for apoA-I, 100:1 for apoA-II, and 35:1 for apoC-I) and incubated for 20 h. The incubation temperature was 24°C for DMPC, 28°C for DMPC:Ch, and 4°C for all DLPC preparations.

In addition, lipoproteins containing these and other lipids (DPPC or POPC) were prepared by sodium cholate dialysis following published protocols (20). Cholesterol-free complexes were prepared using PC:protein:cholate molar ratio of 80:1:80,

and cholesterol-containing complexes were prepared by using PC:Ch:protein molar ratio of 80:4:1. The complexes were isolated by density gradient centrifugation to remove unreacted protein. Briefly, the sample density was adjusted to 1.2 g/ml using solid KBr, the samples were spun at 50,000 rpm at 15°C for 48 h, and the top lipoprotein-containing fraction was collected and dialyzed against the standard buffer. Lipoprotein formation was confirmed by negative staining electron microscopy (EM) and nondenaturing PAGE as described below. Biochemical composition of the reconstituted lipoproteins was determined using Markwell-Lowry assay for protein analysis, Bartlett assay for phospholipids (43), and colorimetric analysis for free cholesterol (44). The PC:Ch ratios in the initial lipid mixture and in rHDL reconstituted from this mixture were similar.

### Gel electrophoresis and EM

Lipoprotein size was assessed by nondenaturing PAGE using 8–25% gradient gels. The samples containing 10 µg protein were run for 2 h at 120 V, the gels were stained with Denville blue protein stain (Denville Scientific), and particle size was assessed from comparison with the high molecular weight standards (GE Healthcare). The results were in good agreement with EM data. For negative staining EM, lipoproteins were visualized under low-dose conditions in a CM12 transmission electron microscope (Philips Electron Optics) as described (40, 41).

### Circular dichroism spectroscopy, 90° light scattering, and lipoprotein stability measurements

Far-UV circular dichroism (CD) data were collected from lipoprotein solutions (20 µg/ml concentration) using an AVIV 215 or AVIV 62DS spectropolarimeter with thermoelectric temperature control. The CD data were normalized to protein concentrations and reported as molar residue ellipticity,  $[\theta]$ . Protein  $\alpha$ -helical content was estimated from the molar residue ellipticity at 222 nm. A fluorescence attachment was used to record 90° light scattering together with the CD signal in thermal denaturation experiments; this enabled us to simultaneously monitor protein unfolding (by CD) and lipoprotein fusion (by light scattering) (45). Earlier thermal denaturation studies of discoidal rHDL showed that apolipoprotein unfolding and dissociation is concomitant with lipoprotein fusion (41); hence, the rates of  $\alpha$ -helical unfolding and particle fusion are similar and provide useful metrics for measuring lipoprotein stability. This does not imply that the particles with higher initial  $\alpha$ -helical content or smaller diameters are necessarily more stable (see Results).

Furthermore, our earlier studies showed that lipoprotein denaturation is a slow thermodynamically irreversible transition involving partial dissociation of the unfolded protein accompanied by disk fusion into protein-containing vesicles (Refs. 40 and 41 and references therein). This necessitates the application of a kinetic, rather than the thermodynamic approach, for quantitative analysis of lipoprotein stability. Still, conventional melting data recorded at a constant scan rate are useful for qualitative analysis, provided that they are recorded at identical heating rates [the melting curves shift to lower temperatures at slower heating rates (40)]. We record such melting data by spectroscopy or calorimetry and use it to establish the relative rank order of lipoprotein stability. For quantitative stability studies, we use kinetic data (which are more sensitive to small changes in stability). The rank orders of particle stability obtained in the melting and kinetic experiments are in good agreement.

In the melting experiments, lipoprotein samples were heated and cooled at a constant rate of 11°C/h, and CD and light scattering data were recorded at 222 nm to monitor  $\alpha$ -helical unfolding and changes in lipoprotein size due to fusion, respectively; the apparent melting temperature  $T_m$  determined under identical

experimental conditions provides a qualitative measure of relative lipoprotein stability. For quantitative kinetic analysis of lipoprotein stability, we used temperature-jump (T-jump) experiments. The sample temperature was rapidly increased at time  $t = 0$  from 25°C to a final constant value ranging from 65–95°C, and the time course of the protein unfolding was monitored by CD at 222 nm,  $\Theta_{222}(t)$ . Importantly, the results of the T-jump experiments did not depend on whether the initial (ambient) temperature was above or below the temperature  $T_c$  of the lipid phase transition. Furthermore, since spontaneous lipoprotein reconstitution (that is fastest near  $T_c$  and rapidly decelerates at higher and lower temperatures) is not detected at the high final temperatures used in our T-jump experiments (65–95°C) (45), the reaction rates measured in these experiments are not affected by reconstitution and reflect solely lipoprotein denaturation. The rates  $k(T)$  of lipoprotein denaturation/protein unfolding at each final temperature were determined from exponential fitting of the  $\Theta_{222}(t)$  data and were used to obtain Arrhenius plots,  $-\ln k(T)$  versus  $1/T$  (which are used to determine the Arrhenius activation energy  $E_a$ ), or their modified versions,  $-RT \ln k(T)$  versus  $1/T$  (which are convenient for determination of free energy changes); both types of plots give similar information on the stability profiles of macromolecules (46). The activation energy (enthalpy)  $E_a \equiv \Delta H^*$  of the denaturation was determined from the slopes of the Arrhenius plots with an accuracy of about  $\pm 5$  kcal/mol, which incorporates the fitting errors and the deviations among different sets of experiments. The shifts in the modified Arrhenius plots were used to determine changes in kinetic stability,  $\Delta G^* = \Delta H^* - T \Delta S^*$ , upon changes in lipoprotein composition,  $\delta \Delta G^*(T) = -RT \delta[\ln k(T)]$  (40); the accuracy of these estimates is about 0.2 kcal/mol. The values of  $E_a$  and  $\delta \Delta G^*$  pertain to mole of cooperative unit in rHDL denaturation, which probably contains one protein and several lipid molecules that dissociate together from the disk (37).

### Differential scanning calorimetry

Excess heat capacity,  $C_p(T)$ , was recorded from lipoprotein solutions (1 mg/ml protein concentration in standard buffer) using an upgraded Microcal MC2 microcalorimeter as described (41). Degassed lipoprotein and/or buffer samples were heated from 5–100°C at a rate 90°C/h, and differential scanning calorimetry (DSC) data were recorded, followed by rapid cooling to 5°C prior to recording the next DSC scan from the same sample. Buffer baselines were subtracted. ORIGIN software was used for the data collection, processing, and display.

All experiments in this work were repeated three or more times to ensure reproducibility.

## RESULTS

### Effects of cholesterol on the structure and stability of apoA-I:PC complexes

Complexes of apoA-I, DMPC, and cholesterol that comprised 0–35 mol% of the total lipid were reconstituted as described in Materials and Methods. Particle size and morphology were assessed by nondenaturing PAGE and negative staining EM (Fig. 1). In the absence of cholesterol, the complexes migrated as a major band with particle size  $\sim 10$  nm (Fig. 1A, lane 0). At 5% cholesterol, an additional band of larger particles (12–13 nm) was observed (lane 5), and at 10% cholesterol, the particle size in the major band further increased to about 17 nm, which is within the range typical of rHDL disks (lane 10). This was accompanied by the formation of uncomplexed apoA-I (lanes 5 and 10).

From 15% onwards, a disappearance of discoidal particles with the formation of vesicles and dissociated lipid-free protein was observed (Fig. 1A, lanes 15–30). EM data agreed with the PAGE results and showed discoidal particles (stacked on edge or face up) whose diameter increased upon raising cholesterol concentration from 0–10 mol% (Fig. 1B–D). At 15 mol% cholesterol and above, larger particles were formed whose diameter ( $>22$  nm) and morphology were typical of collapsed vesicles (Fig. 1E, F). This is consistent with the earlier studies reporting formation of larger particles at higher cholesterol concentrations (24, 25). Our results also show that the standard apoA-I:DMPC:Ch preparations containing 0–10 mol% cholesterol yield discoidal rHDL, while those containing 15 mol% cholesterol and above yield vesicular complexes.

For spectroscopic studies, the apoA-I:DMPC:Ch complexes were isolated by density centrifugation as described in Materials and Methods; this led to the complete removal of the uncomplexed protein without changing the particle size or morphology (as confirmed by nondenaturing PAGE and EM; data not shown). Far-UV CD spectra of the isolated complexes (data not shown) were consistent with the earlier reports (21) and showed a small gradual reduction in CD amplitude at 222 nm and other wavelengths, indicating up to 15% reduction in the protein  $\alpha$ -helical content upon increasing cholesterol content from 0–35 mol%. Thermal stability of the complexes was assessed by CD spectroscopy in melting and kinetic experiments (Fig. 2). Fig. 2A shows CD melting data,  $\Theta_{222}(T)$ , recorded at 222 nm to monitor  $\alpha$ -helical unfolding/refolding during particle heating/cooling at a constant rate of 11°C/h. Earlier studies showed that rHDL heating leads to protein unfolding and partial dissociation accompanied by disk fusion into vesicles [(41); also see Fig. 3A below]; hence, we monitored protein unfolding to assess particle stability. The heating data,  $\Theta_{222}(T)$ , of the complexes containing 0–10 mol% cholesterol largely overlapped (solid lines, Fig. 2A), suggesting similar stability. However, the heating data recorded of the complexes containing 15 mol% and above shifted to lower temperatures (dashed lines), suggesting reduced stability. This was confirmed in T-jumps to 80°C (Fig. 2B) and other temperatures: kinetic CD data,  $\Theta_{222}(t)$ , of the disks containing 0–10% cholesterol largely overlapped (solid lines, Fig. 2B), indicating similar unfolding rates  $k(T)$  [and, hence, similar kinetic stability  $\Delta G^*(T) \propto -RT \cdot \ln k(T)$ ], while at higher cholesterol concentrations, faster unfolding (and, hence, lower stability) was detected (dashed lines). In summary, increasing cholesterol content in apoA-I:DMPC complexes from 0–35 mol% leads to a large increase in the particle diameter and a small reduction in the protein  $\alpha$ -helical content; the disk stability does not significantly change upon increasing cholesterol content from 0–10 mol%, yet further increase to 15 mol% and above leads to formation of protein-containing vesicles that are less stable than the disks.

Does disk-to-vesicle conversion by other factors also reduce the particle stability? Heating of apoC-I:DMPC or apoA-II:DMPC disks led to their fusion into protein-containing vesicles (40, 41) that were apparently less stable than the disks, as suggested by faster protein unfolding ob-

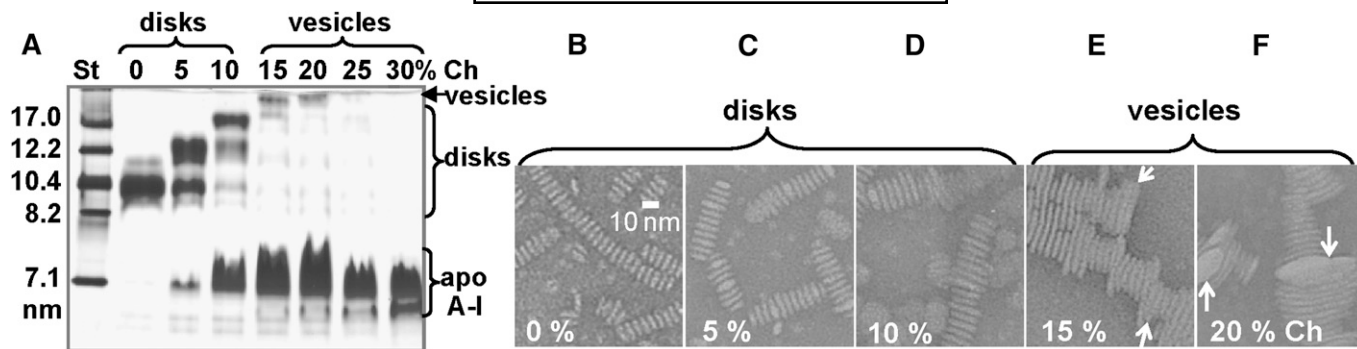


**Fig. 1.** Effect of cholesterol on the size and morphology of apoA-I:DMPC:Ch complexes. The complexes were reconstituted from human apoA-I, DMPC, and cholesterol as described in Materials and Methods. A: Nondenaturing PAGE (8–25% gradient, Denville blue staining). B–F: Electron micrographs of negatively stained complexes. Cholesterol content (0–35 mol% of the total lipid) is indicated; PAGE data for 25, 30 (A), and 35% cholesterol (data not shown) are similar; EM data for 20% (F) and higher cholesterol concentrations (data not shown) are similar. White arrows in E and F indicate rounded edges in the lamellar stacks (E) and large elongated particles (F) characteristic of collapsed vesicles.

served upon repeated heating and cooling (40). Repeated heating and cooling of apoA-I:DMPC complexes (Fig. 3) confirmed this notion. Nondenaturing PAGE showed that heating converted intact disks to protein-containing vesicles and dissociated protein (Fig. 3A). Disk-to-vesicle conversion was also evident from the DSC data recorded in repetitive scans of the same sample (Fig. 3B, solid and dashed lines): the first heating scan showed a relatively broad gel-to-liquid crystal phase transition centered at 26°C, which is characteristic of discoidal rHDL, whereas the second scan showed a sharper transition (reflecting larger cooperative unit) that was shifted to  $T_c = 24^\circ\text{C}$ , which is characteristic of DMPC vesicles (47). Furthermore, compared with the first heating scan, consecutive heating scans monitored by DSC and CD resulted in lower apparent melting temperature  $T_m$  (Fig. 3B, C) and faster protein unfolding (Fig. 3D), indicating reduced stability. These results consistently show that, for the complexes comprised of similar proteins and lipids, the disks are more stable than the vesicles.

Next, we tested whether cholesterol affects the stability of discoidal complexes of apoA-I with other PCs, including physiologic PCs [most of which contain 16 to 18 carbons in their acyl chains with one or more double bonds in sn-2 position (48)]. Discoidal complexes of apoA-I with POPC (16:0,18:1) or DPPC (16:0,16:0) and 0–10 mol% cholesterol were reconstituted and analyzed by nondenaturing PAGE, EM, and CD in melting and kinetic experiments. The results (see supplementary data) were similar to those of apoA-I:DMPC:Ch disks (Figs. 1, 2) and showed that increasing cholesterol content from 0 to 10 mol% caused no detectable changes in the disk stability. In summary, increasing cholesterol content from 0–10 mol% in discoidal complexes of apoA-I with DMPC, POPC, or DPPC has no significant effect on the disk stability.

#### Effects of cholesterol on the stability of apoA-II:PC complexes

To test whether cholesterol affects the stability of PC complexes with other exchangeable apolipoproteins, we analyzed rHDL disks containing the second major HDL

protein, human apoA-II. Earlier studies of binary DMPC complexes with human apoA-I (243 amino acids), apoA-II (S-S linked dimer of two 77 amino acid molecules), and apoC-I (57 amino acids) showed that the rank order of the disk stability correlates with the protein size,  $A-I > A-II_{\text{dimer}} > A-II_{\text{monomer}} > C-I$  (41). Thus, the disks containing apoA-II are less stable than those with apoA-I. Fig. 4 shows the data recorded of apoA-II:DMPC disks containing 0–10% cholesterol. Nondenaturing PAGE (Fig. 4A) and EM data (data not shown) of apoA-II:DMPC disks demonstrate that increasing cholesterol content leads to formation of larger disks; thus, increasing cholesterol from 0 to 10 mol% increases the particle size in the major band from about 10.5 to 18 nm (Fig. 4A). Cholesterol incorporation in the disks was accompanied by a small reduction in the  $\alpha$ -helical content of apoA-II evident from a small reduction in CD amplitude at 222 nm and other wavelengths, which had little, if any, destabilizing effect on the disks. In fact, the disks containing 0 and 10% cholesterol showed *i)* similar appar-

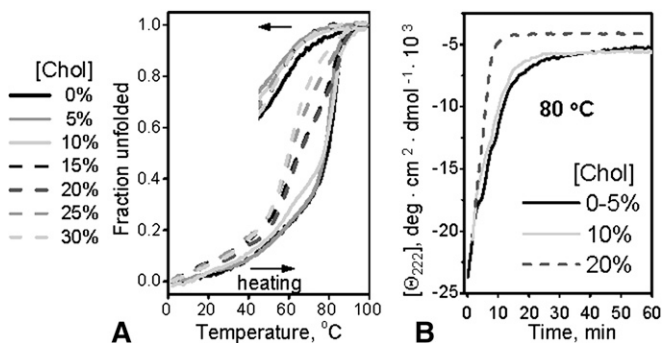


**Fig. 2.** Thermal denaturation of apoA-I:DMPC:Ch complexes. The complexes were reconstituted as described in Materials and Methods; cholesterol content (mol% of the total lipid) is indicated. Protein unfolding during thermal denaturation was monitored by CD at 222 nm in melting (A) and kinetic (B) experiments. A: Melting data (normalized to fraction unfolded) recorded during sample heating and cooling at a rate of 11°C/h; arrows show directions of the temperature changes. B: Kinetic data recorded in T-jumps from 25–80°C.

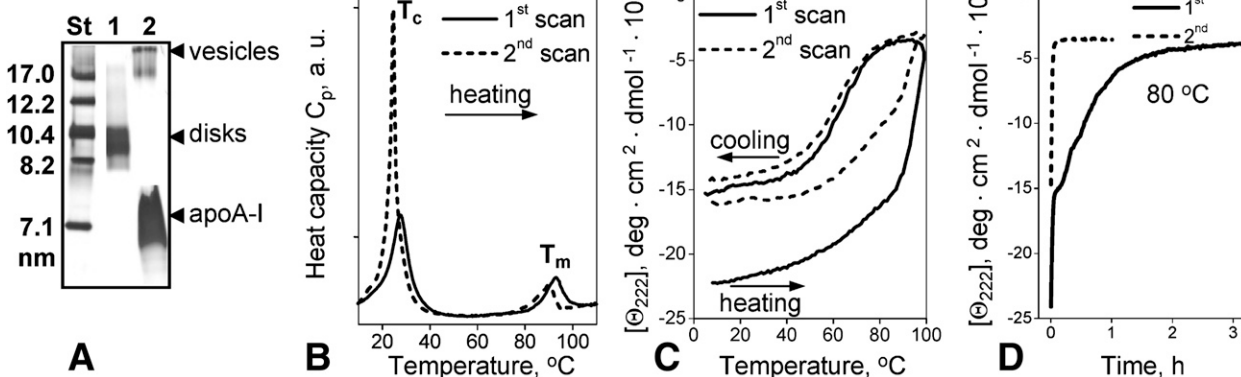


**Fig. 3.** Effects of consecutive heating and cooling on thermal denaturation of apoA-I:DMPC complexes. Intact discoidal complexes were denatured by heating (first scan, solid lines), followed by cooling below 24°C and immediate heating (second scan, dashed lines). **A:** Nondenaturing PAGE of discoidal complexes before (lane 1) or immediately after completion of the first calorimetric scan to 100°C (lane 2) shows protein dissociation and disk-to-vesicle conversion upon heating. **B:** Thermal denaturation monitored by differential scanning calorimetry during heating at 90°C/h. The peak centered at  $T_c$  reflects endothermic gel-to-liquid crystal phase transition in DMPC; while that at  $T_m$  reflects lipoprotein denaturation. The spacing between the y axis ticks corresponds to 50 kcal/mole (protein)·K. **C:** Melting data recorded by CD at 222 nm for protein unfolding/refolding upon consecutive heating and cooling at 11°C/h rate; the directions of the temperature changes are indicated. **D:** Kinetic CD data recorded in consecutive T-jumps from 25–80°C.

ent melting temperatures  $T_m$  assessed by CD at 222 nm for  $\alpha$ -helical unfolding and by 90° light scattering for increase in the particle size upon fusion (Fig. 4B, C), and *ii*) similar protein unfolding rates measured by CD in T-jumps (Fig. 4D). Discoidal complexes of apoA-II with other PCs, including POPC, also showed no significant effects of cholesterol on the disk stability (data not shown). Thus, similar to apoA-I, the disks containing apoA-II showed a sizable increase in diameter and a small reduction in protein  $\alpha$ -helical content but no significant changes in disk stability upon incorporation of 10 mol% cholesterol.

#### Effects of cholesterol on the stability of apoC-I:PC complexes

Next, we tested the effects of cholesterol on the PC complexes with human apoC-I. **Fig. 5** shows the results for apoC-I:DMPC complexes. EM data demonstrate that the

disk diameter did not significantly change upon incorporation of up to 10 mol% cholesterol, but increasing cholesterol content to 20 mol% and beyond led to an increase in diameter (Fig. 5A). Furthermore, similarly to apoA-I and apoA-II, the apoC-I-containing complexes changed their morphology from disks (at 0–10 mol% cholesterol) to vesicles (at and above 20 mol% cholesterol) (Fig. 5A). In contrast to apoA-I or apoA-II, the melting and kinetic data of apoC-I:DMPC disks revealed increased stability upon increasing cholesterol concentration from 0–10 mol% evident from higher apparent melting temperature and slower protein unfolding (solid black and gray lines, Fig. 5B, C). Further increase in cholesterol, from 10% (in disks) to 20% (in small vesicles), led to no large changes in stability, as indicated by the overlapping melting curves and kinetic data recorded at 10% and 20% cholesterol (solid gray and dashed black lines in Fig. 5B, C). An in-

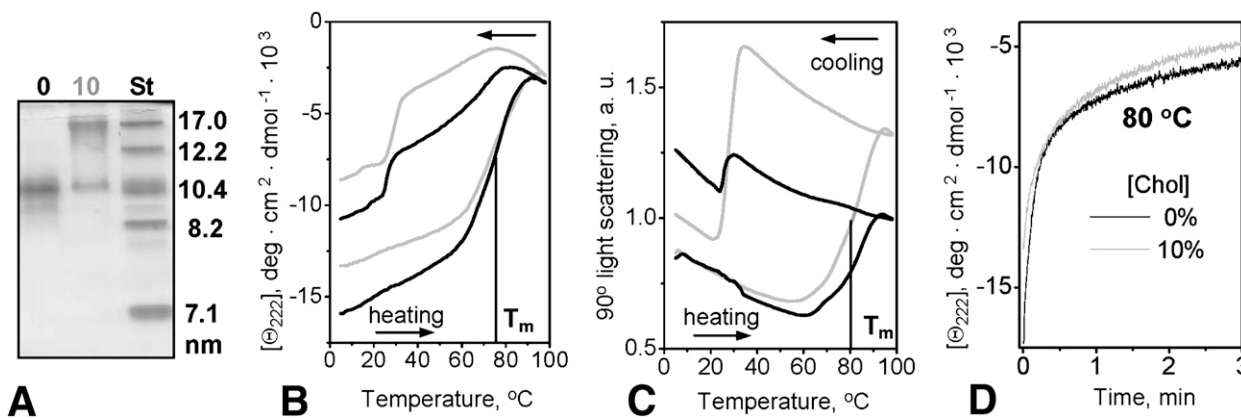


**Fig. 4.** Effects of cholesterol on size and stability of apoA-II:DMPC disks. Complexes of human apoA-II and DMPC containing 0% (black) or 10 mol% cholesterol (gray) were reconstituted as described in Materials and Methods. **A:** Nondenaturing PAGE (8–25% gradient, Denville blue staining) of the complexes; cholesterol content is indicated on the lanes. Thermal denaturation monitored at 222 nm by CD spectroscopy (**B**) and 90° light scattering (**C**) upon sample heating/cooling at a rate of 11°C/h. **D:** Thermal denaturation monitored by CD at 222 nm in a T-jump from 25–80°C.

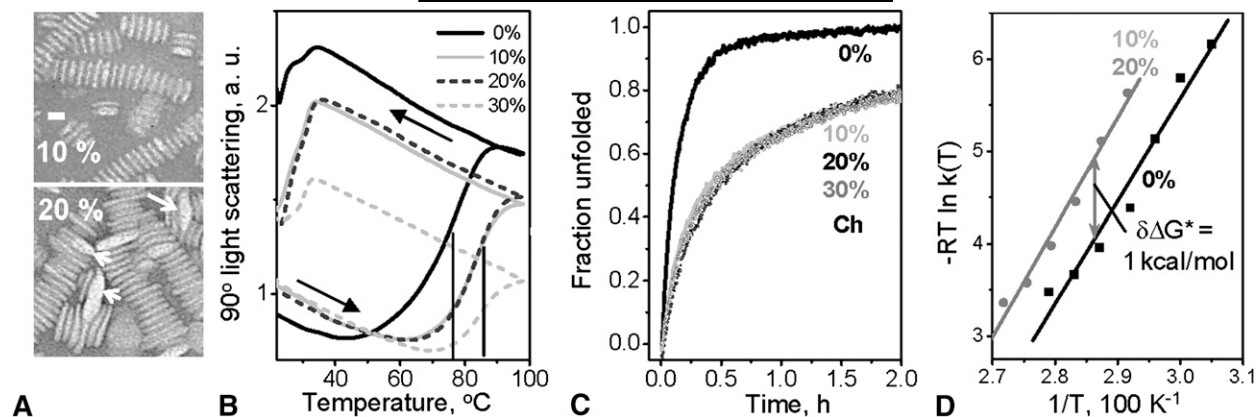


**Fig. 5.** Effects of cholesterol on the size and stability of apoC-I:DMPC:Ch complexes. **A:** Electron micrographs of the negatively stained complexes containing 0–10 mol% (disks, top panel) or 20 mol% cholesterol (vesicles, bottom panel). White arrows in the bottom panel indicate stacks of particles with rounded edges, distorted stacks, and large elongated particles characteristic of collapsed vesicles. Bar size is 10 nm. **B:** Changes in the particle size monitored by 90° light scattering at 222 nm during heating and cooling from 20–98°C at a rate of 11°C/h; cholesterol content in the complexes was 0 (black solid), 10 (gray solid), 20 (black dashed), or 30 mol% (gray dashed). Arrows show directions of the temperature changes; negative slopes in the melting data result from an optical artifact of the CD instrument (45). Vertical lines indicate apparent melting temperatures  $T_m$ . **C:** Protein unfolding monitored by CD at 222 nm in T-jumps from 25–80°C; the data are normalized to fraction unfolded; cholesterol content in the complexes is indicated. **D:** Arrhenius plots obtained from the kinetic CD data, such as those in C, recorded in T-jumps from 25°C to various final temperatures  $T$  at each temperature were obtained by monoexponential fitting of the CD data,  $\Theta_{222}(t) = A \exp(-k(T)t)$ , where  $A$  is the amplitude and  $k$  is the rate of the CD changes. The nearly parallel shift in the Arrhenius plots observed upon increasing cholesterol content from 0 to 10 or 20 mol% (double arrow) corresponds to an increase in kinetic lipoprotein stability by about  $\delta\Delta G^* = 1 \pm 0.2$  kcal/mol.

crease from 20% to 30% cholesterol led to no large additional stabilization (dashed lines). Taken together, these results suggest that increasing cholesterol content from 0–10 mol% stabilizes the apoC-I:DMPC disks, but at 20 mol% and higher cholesterol concentrations, this effect is offset by the particle destabilization upon disk-to-vesicle conversion.

To quantify cholesterol-induced stabilization of apoC-I:DMPC disks, we carried out Arrhenius analysis of the T-jump CD data that were recorded from these disks containing 0% (40) or 10% cholesterol data not shown) at several temperatures ranging from 65–95°C. The  $\Theta_{222}(t)$  data at each temperature  $T$  were approximated with monoexponentials,  $\Theta_{222}(t) = A \exp(-k(T)t)$ , where  $A$  is the amplitude and  $k(T)$  is the unfolding rate. The Arrhenius plots,  $-RT \ln k(T)$  versus  $1/T$ , for the disks containing 0% and 10% cholesterol were parallel with slopes corresponding to the activation energy of disk denaturation  $E_a = 25 \pm 5$  kcal/mol (Fig. 5D). The shift between these plots indicates an increase in the kinetic disk stability by  $\delta\Delta G^* = -\delta[RT \ln k(T)] = 1.1 \pm 0.2$  kcal/mol upon increasing cholesterol content from 0% to 10 mol% (Fig. 5D, vertical arrow). The errors in these estimates reflect the fitting errors and the deviations among different data sets. Limited accuracy in  $E_a$  determination ( $\pm 5$  kcal/mol) prevents us from determining whether the cholesterol-induced disk stabilization by  $\delta\Delta G^* \sim 1$  kcal/mol is an enthalpic or entropic effect.

To test whether cholesterol stabilizes other apoC-I:PC disks, we carried out thermal denaturation studies of such disks containing 0% or 10% cholesterol and DLPC (12:0,12:0), DPPC (16:0,16:0), or POPC (16:0,18:1) (data not shown). Earlier studies of the binary complexes

of apoC-I with these PCs showed that the kinetic disk stability,  $\Delta G^* = \Delta H^* - T\Delta S^*$ , and its enthalpic component,  $\Delta H^* \cong E_a$ , increase linearly with increasing acyl chain length and that the cis-double bond in POPC is destabilizing; thus, the rank order of the disk stability is DLPC < DMPC, POPC < DPPC (37). EM data of this study show that the complexes containing up to 10% cholesterol had discoidal morphology. Thermal denaturation studies, which used CD and 90° light scattering in melting and kinetic experiments, showed that incorporation of 10 mol% cholesterol led to a small but significant stabilization of the apoC-I:DLPC disks by about 0.5 kcal/mol; however, no cholesterol-induced changes in stability were detected in the disks containing apoC-I and DPPC or POPC (data not shown). Taken together, our results suggest that incorporation of 10 mol% cholesterol tends to stabilize less stable disks (apoC-I:DLPC and apoC-I:DMPC) but not the more stable complexes (apoC-I:DPPC, apoC-I:POPC, and any complexes containing apoA-I or apoA-II). Thus, reduction in acyl chain fluidity upon cholesterol incorporation does not necessarily lead to increased rHDL stability.

## DISCUSSION

### Effects of cholesterol on rHDL stability: correlation with electrostatic effects

This work reports the first kinetic analysis of the effects of cholesterol on the thermal stability of discoidal rHDL. The results reveal that these effects depend on the lipoprotein composition and correlate inversely with the lipoprotein stability. Cholesterol tends to stabilize less stable complexes (such as apoC-I with shorter-chain lipids,

DMPC, or DLPC; Fig. 5) but has no large effect on the more stable complexes (such as the disks containing either larger proteins, apoA-II, or apoA-I, and/or longer-chain lipids, POPC, or DPPC, and up to 10 mol % cholesterol; solid lines in Fig. 2; Fig. 5) and may even destabilize these complexes at or above 15 mol% (Fig. 2, dashed lines). Interestingly, a similar trend was observed in our earlier studies of the electrostatic interactions that play a major role in HDL stability (49, 50): salt stabilizes less stable complexes, apparently by ionic screening of unfavorable electrostatic interactions among the protein charges; however, in more stable complexes, where the electrostatic interactions are better optimized, the effects of salt on the lipoprotein stability decrease and eventually change sign (49). This similarity suggests that the effects of cholesterol on rHDL stability may originate, in part, from altered electrostatic interactions resulting from an increased net negative charge on HDL upon pK normalization in lysines (21). Cholesterol-induced effects on the protein and lipid packing interactions and on the void volume of the PC bilayer are other factors that may affect the disk stability. Furthermore, the effects of salt and cholesterol on rHDL stability may illustrate a general trend: for a series of homologous macromolecules or their complexes, various external (solvent ionic conditions) or internal (cholesterol) factors may enhance favorable interactions in relatively unstable systems, yet in more stable systems, where such interactions are already highly optimized, the effect of these factors is diminished or even becomes destabilizing (Ref. 49 and references therein).

#### Comparison with the effects of cholesterol on integral membrane proteins

Effects of cholesterol on the structure, dynamics, and function of integral membrane proteins have been intensely investigated and are distinctly different from those observed in apolipoproteins. In contrast to apolipoprotein:PC complexes that may be either stabilized or destabilized by cholesterol (Figs. 2, 4, and 5), integral membrane proteins show increased structural stability upon cholesterol incorporation into a phospholipid bilayer (Refs. 1, 50, and references therein). This increased stability (which is attributed to reduced void volume in a cholesterol-containing bilayer) has been linked to reduced conformational flexibility that is often necessary for protein function; as a result, the function of membrane proteins, such as rhodopsins, is impaired by high cholesterol concentrations in the bilayer (50). In contrast, in amphipathic apolipoprotein  $\alpha$ -helices bound at the lipid surface, cholesterol incorporation does not necessarily increase the stability of the protein:lipid complex or reduce its structural flexibility. As a result, cholesterol does not necessarily stabilize apolipoproteins (such as apoA-I and apoA-II; Figs. 2, 4) on HDL surface or reduce structural flexibility of this surface, which is required for metabolic HDL remodeling (Ref. 38 and references therein). This may explain why cholesterol incorporation does not impair HDL function in RCT despite reduction in chain fluidity.


Other effects of cholesterol on the structure and function of membrane proteins involve direct sterol-protein interactions as well as indirect effects, such as increase in the bilayer thickness due to straightening of the acyl chains, which may cause a mismatch between the hydrophobic thickness of the bilayer and the protein (1, 6). These effects are unlikely to provide a dominant contribution to rHDL stability and function for the following reasons. First, most studies of discoidal rHDL showed that cholesterol is preferentially excluded from the protein-lipid boundary (Refs. 27–30 and references therein); thus, even though direct apolipoprotein-sterol interactions cannot be excluded, they are unlikely to provide a major contribution to lipoprotein stability. Second, in contrast to membrane proteins whose function is optimized for the physiologic bilayer thickness, rHDL function in cholesterol uptake and esterification improves for nonphysiologic shorter-chain PCs, and this functional improvement is paralleled by a reduction in rHDL stability upon reduction in the disk thickness (37). Thus, possible increase in the disk thickness upon cholesterol incorporation may not cause a hydrophobic mismatch between apolipoprotein and lipid. Our results also show that thicker cholesterol-containing disks are not necessarily more stable than their thinner cholesterol-free counterparts (Figs. 2, 4). Furthermore, the observation that cholesterol stabilizes DMPC complexes with apoC-I but destabilizes similar complexes with apoA-I (Figs. 2, 5) suggests that the effects of cholesterol on rHDL are not due to specific sterol-PC interactions. Taken together, our results suggest that the effects of cholesterol on rHDL stability are dominated by the overall changes in the lipoprotein packing (such as changes in the PC head group spacing and acyl chain tilt in the protein charge distribution and  $\alpha$ -helical content, etc.) rather than specific interactions of sterol with individual protein or PC moieties or sterol-induced increase in the hydrophobic thickness of the disk.

#### Molecular mechanism and biological relevance

Our results show that the amount of cholesterol that can be packed in rHDL varying in protein and PC composition (up to  $\sim$ 10 mol% cholesterol in disks and up to 35 mol% in vesicles; Fig. 1) is comparable to that in nascent HDL (whose cholesterol content typically ranges from 4–10 mol% and does not exceed 20 mol%; 14–16). This inability of discoidal particles to accommodate more than 10 mol% cholesterol may help explain why cholesterol concentration in nascent HDL is much lower than that in the plasma membrane from which these particles are formed ( $\sim$ 40 mol%). The resulting gradient favors cholesterol movement from plasma membrane to HDL during RCT. The reason why this limited amount of cholesterol can be packed in HDL is unclear; one possibility is preferential exclusion of cholesterol from apolipoproteins and their adjacent PCs that comprise a large fraction of all HDL PCs [55% according to (28)], leading to a high local concentration of cholesterol in the middle of the disk.

In summary, our studies of rHDL comprised of apoA-I and various PCs including POPC, which mimic the compo-



sition of nascent HDL, reveal that the stability of these rHDL (and, by inference, of nascent HDL) is nearly invariant or decreases with increasing cholesterol content (see supplementary data and Fig. 2). This helps explain earlier rHDL studies showing that increasing cholesterol content does not impair and may even improve the functions of apoA-I in nascent HDL despite reduced chain fluidity (31, 32). Consistent with this notion, <sup>31</sup>P NMR studies of PC bilayers showed that, even at 30 mol%, cholesterol has only modest effects on the orientation and mobility of phospholipid head groups in liquid phase and does not order them as it orders the hydrocarbon chains (51, 52). We speculate that, in nascent HDL, cholesterol has little ordering effect on the PC head groups and is largely excluded from the protein-containing disk periphery. As a result, cholesterol has no large effect on the structural disorder in lipoprotein surface, which, we postulate, is essential for insertion of LCAT and other plasma factors during HDL remodeling in RCT (38). Taken together, these results support our hypothesis that the localized structural disorder in the lipoprotein surface, which is inversely related to lipoprotein stability (38), provides a better determinant of functional HDL remodeling than chain fluidity. This notion probably applies to discoidal as well as spherical HDL whose functional remodeling by plasma factors (such as LCAT and cholesterol ester and phospholipid transfer proteins) involves protein dissociation and particle fusion and hence depends upon particle stability (38, 53–56). 

The authors thank Dr. Henry Pownall for his generous gift of human plasma apoA-II. We are indebted to Dr. Michael Oda for providing the apoA-I bacterial expression system that was used as a control at the final stages of this project. We thank Dr. Giorgio Cavigliolo for technical help and useful discussions. We also thank Cheryl England and Michael Gigliotti for assistance with lipoprotein and apolipoprotein isolation. Last but not least, we thank Dr. Mary F. Roberts for very useful discussion of cholesterol effects on the PC head group dynamics.

## REFERENCES

- Yeagle, P. L. 1991. Modulation of membrane function by cholesterol. *Biochimie*. **73**: 1303–1310.
- Mouritsen, O. G., and M. J. Zuckermann. 2004. What's so special about cholesterol? *Lipids*. **39**: 1101–1113.
- Róg, T., M. Pasenkiewicz-Gierula, I. Vattulainen, and M. Karttunen. 2009. Ordering effects of cholesterol and its analogues. *Biochim. Biophys. Acta*. **1788**: 97–121.
- Churchward, M. A., T. Rogasevskaia, D. M. Brandman, H. Khosravani, P. Nava, J. K. Atkinson, and J. R. Coorsen. 2008. Specific lipids supply critical negative spontaneous curvature – an essential component of native Ca<sup>2+</sup>-triggered membrane fusion. *Biophys. J.* **94**: 3976–3986.
- Biswas, S., S. R. Yin, P. S. Blank, and J. Zimmerberg. 2008. Cholesterol promotes hemifusion and pore widening in membrane fusion induced by influenza hemagglutinin. *J. Gen. Physiol.* **131**: 503–513.
- Lundbaek, J. A., O. S. Andersen, T. Werge, and C. Nielsen. 2003. Cholesterol-induced protein sorting: an analysis of energetic feasibility. *Biophys. J.* **84**: 2080–2089.
- Brown, M. S., and J. L. Goldstein. 2009. Cholesterol feedback: from Schoenheimer's bottle to Scap's MELADL. *J. Lipid Res.* **50** (Suppl.): S15–S27.

- Rader, D. J., E. T. Alexander, G. L. Weibel, J. Billheimer, and G. H. Rothblat. 2009. Role of reverse cholesterol transport in animals and humans and relationship to atherosclerosis. *J. Lipid Res.* **50** (Suppl.): S189–S194.
- Lee, J. Y., and J. S. Parks. 2005. ATP-binding cassette transporter AI and its role in HDL formation. *Curr. Opin. Lipidol.* **16**: 19–25.
- Oram, J. F., and J. W. Heinecke. 2005. ATP-binding cassette transporter AI: a cell cholesterol exporter that protects against cardiovascular disease. *Physiol. Rev.* **85**: 1343–1372.
- Davidson, W. S., and T. B. Thompson. 2007. The structure of apolipoprotein A-I in high density lipoproteins. *J. Biol. Chem.* **282**: 22249–22253.
- Silva, R. A., R. Huang, J. Morris, J. Fang, E. O. Gracheva, G. Ren, A. Kontush, W. G. Jerome, K. A. Rye, and W. S. Davidson. 2008. Structure of apolipoprotein A-I in spherical high density lipoproteins of different sizes. *Proc. Natl. Acad. Sci. USA.* **105**: 12176–12181.
- Chen, B., X. Ren, T. Neville, W. G. Jerome, D. W. Hoyt, D. Sparks, G. Ren, and J. Wang. 2009. Apolipoprotein AI tertiary structures determine stability and phospholipid-binding activity of discoidal high-density lipoprotein particles of different sizes. *Protein Sci.* **18**: 921–935.
- Skipsky, V. P. 1979. Lipid composition in lipoproteins in normal and diseased states. In *Blood Lipids and Lipoproteins: Quantitation, Composition and Metabolism*. G. J. Nelson, editor. R.E. Krieger Publishing Company, Huntington, NY. 471–583.
- Duong, P. T., H. L. Collins, M. Nickel, S. Lund-Katz, G. H. Rothblat, and M. C. Phillips. 2006. Characterization of nascent HDL particles and microparticles formed by ABCA1-mediated efflux of cellular lipids to apoA-I. *J. Lipid Res.* **47**: 832–843.
- Mulya, A., J. Y. Lee, A. K. Gebre, M. J. Thomas, P. L. Colvin, and J. S. Parks. 2007. Minimal lipidation of pre-beta HDL by ABCA1 results in reduced ability to interact with ABCA1. *Arterioscler. Thromb. Vasc. Biol.* **27**: 1828–1836.
- Baldán, A., P. Tarr, R. Lee, and P. A. Edwards. 2006. ATP-binding cassette transporter G1 and lipid homeostasis. *Curr. Opin. Lipidol.* **17**: 227–232.
- Barter, P. J. 2002. Hugh Sinclair Lecture: The regulation and remodeling of HDL by plasma factors. *Atheroscler. Suppl.* **3**: 39–47.
- Zannis, V. I., A. Chroni, and M. Krieger. 2006. Role of apoA-I, ABCA1, LCAT, and SR-BI in the biogenesis of HDL. *J. Mol. Med.* **84**: 276–294.
- Jonas, A. 1986. Reconstitution of high-density lipoproteins. *Methods Enzymol.* **128**: 553–582.
- Sparks, D. L., W. S. Davidson, S. Lund-Katz, and M. C. Phillips. 1993. Effect of cholesterol on the charge and structure of apolipoprotein A-I in recombinant high density lipoprotein particles. *J. Biol. Chem.* **268**: 23250–23257.
- Bergeron, J., P. G. Frank, D. Scales, Q. H. Meng, G. Castro, and Y. L. Marcel. 1995. Apolipoprotein A-I conformation in reconstituted discoidal lipoproteins varying in phospholipid and cholesterol content. *J. Biol. Chem.* **270**: 27429–27438.
- Kono, M., Y. Okumura, M. Tanaka, D. Nguyen, P. Dhanasekaran, S. Lund-Katz, M. C. Phillips, and H. Saito. 2008. Conformational flexibility of the N-terminal domain of apolipoprotein A-I bound to spherical lipid particles. *Biochemistry*. **47**: 11340–11347.
- Arnulphi, C., L. Jin, M. A. Triccerri, and A. Jonas. 2004. Enthalpy-driven apolipoprotein A-I and lipid bilayer interaction indicating protein penetration upon lipid binding. *Biochemistry*. **43**: 12258–12264.
- Massey, J. B., and H. J. Pownall. 2008. Cholesterol is a determinant of the structures of discoidal high density lipoproteins formed by the solubilization of phospholipid membranes by apolipoprotein A-I. *Biochim. Biophys. Acta*. **1781**: 245–253.
- Saito, H., Y. Miyako, T. Handa, and K. Miyajima. 1997. Effect of cholesterol on apolipoprotein A-I binding to lipid bilayers and emulsions. *J. Lipid Res.* **38**: 287–294.
- Egashira, M., G. Gorbenko, M. Tanaka, H. Saito, J. Molotkovsky, M. Nakano, and T. Handa. 2002. Cholesterol modulates interaction between an amphipathic class A peptide, Ac-18A-NH<sub>2</sub>, and phosphatidylcholine bilayers. *Biochemistry*. **41**: 4165–4172.
- Tall, A. R., and Y. Lange. 1978. Interaction of cholesterol, phospholipid and apoprotein in high density lipoprotein recombinants. *Biochim. Biophys. Acta*. **513**: 185–197.
- Massey, J. B., H. S. She, A. M. Gotto, Jr., and H. J. Pownall. 1985. Lateral distribution of phospholipid and cholesterol in apolipoprotein A-I recombinants. *Biochemistry*. **24**: 7110–7116.

30. Dergunov, A. D., G. E. Dobretsov, S. Visvikis, and G. Siest. 2001. Protein-lipid interactions in reconstituted high density lipoproteins: apolipoprotein and cholesterol influence. *Chem. Phys. Lipids*. **113**: 67–82.
31. Pownall, H. J., Q. Pao, and J. B. Massey. 1985. Acyl chain and head-group specificity of human plasma lecithin:cholesterol acyltransferase. Separation of matrix and molecular specificities. *J. Biol. Chem.* **260**: 2146–2152.
32. Sparks, D. L., G. M. Anantharamaiah, J. P. Segrest, and M. C. Phillips. 1995. Effect of the cholesterol content of reconstituted LpA-I on lecithin:cholesterol acyltransferase activity. *J. Biol. Chem.* **270**: 5151–5157.
33. Davidson, W. S., K. L. Gillotte, S. Lund-Katz, W. J. Johnson, G. H. Rothblat, and M. C. Phillips. 1995. The effect of high density lipoprotein phospholipid acyl chain composition on the efflux of cellular free cholesterol. *J. Biol. Chem.* **270**: 5882–5890.
34. Parks, J. S., K. W. Huggins, A. K. Gebre, and E. R. Bursleson. 2000. Phosphatidylcholine fluidity and structure affect lecithin:cholesterol acyltransferase activity. *J. Lipid Res.* **41**: 546–553.
35. Kontush, A., P. Therond, A. Zerrad, M. Couturier, A. Nègre-Salvyre, J. A. de Souza, S. Chantepie, and M. J. Chapman. 2007. Preferential sphingosine-1-phosphate enrichment and sphingomyelin depletion are key features of small dense HDL<sub>3</sub> particles: relevance to antiapoptotic and antioxidative activities. *Arterioscler. Thromb. Vasc. Biol.* **27**: 1843–1849.
36. Massey, J. B., and H. J. Pownall. 2005. Role of oxysterol structure on the microdomain-induced microsomalubilization of phospholipid membranes by apolipoprotein A-I. *Biochemistry*. **44**: 14376–14384.
37. Guha, M., D. L. Gantz, and O. Gursky. 2008. Effect of fatty acyl chain length, unsaturation and pH on the stability of discoidal high-density lipoproteins. *J. Lipid Res.* **49**: 1752–1761.
38. Guha, M., X. Gao, S. Jayaraman, and O. Gursky. 2008. Correlation of structural stability and functional remodeling of high-density lipoproteins: The importance of being disordered. *Biochemistry*. **47**: 11393–11397.
39. Gao, X., S. Yuan, S. Jayaraman, and O. Gursky. 2009. Differential stability of high-density lipoprotein subclasses: effects of particle size and protein composition. *J. Mol. Biol.* **387**: 628–638.
40. Gursky, O., Ranjana, and Gantz, D. L. 2002. Complex of human apolipoprotein C-1 with phospholipid: thermodynamic or kinetic stability? *Biochemistry*. **41**: 7373–7384.
41. Jayaraman, S., D. L. Gantz, and O. Gursky. 2005. Kinetic stabilization and fusion of apolipoprotein A-2:DMPC disks: comparison with apoA-1 and apoC-1. *Biophys. J.* **88**: 2907–2918.
42. Ryan, R. O., T. M. Forte, and M. N. Oda. 2003. Optimized bacterial expression of human apolipoprotein AI. *Protein Expr. Purif.* **27**: 98–103.
43. Bartlett, G. R. 1959. Phosphorous assay in column chromatography. *J. Biol. Chem.* **234**: 466–468.
44. Zack, B., N. Moss, A. S. Boyle, and A. Zlatkis. 1954. Reaction of certain unsaturated steroids with acid iron reagent. *Anal. Chem.* **26**: 776–777.
45. Benjwal, S., S. Verma, K. H. Röhm, and O. Gursky. 2006. Monitoring protein aggregation during thermal unfolding in circular dichroism experiments. *Protein Sci.* **15**: 635–639.
46. Schellman, J. A. 1997. Temperature, stability, and the hydrophobic interaction. *Biophys. J.* **73**: 2960–2964.
47. Shaw, A. W., McLean, M. A., and Sligar, S. G. 2004. Phospholipid phase transitions in homogeneous nanometer scale bilayer discs. *FEBS Lett.* **556**: 260–264.
48. Skipski, V. P., M. Barclay, R. K. Barclay, V. A. Fetzer, J. J. Good, and F. M. Archibald. 1967. Lipid composition of human serum lipoproteins. *Biochem. J.* **104**: 340–352.
49. Benjwal, S., S. Jayaraman, and O. Gursky. 2005. Electrostatic effects on the kinetic stability of model discoidal high-density lipoproteins. *Biochemistry*. **44**: 10218–10226.
50. Albert, A. D., K. Boesze-Battaglia, Z. Paw, A. Watts, and R. M. Epand. 1996. Effect of cholesterol on rhodopsin stability in disk membranes. *Biochim. Biophys. Acta.* **1297**: 77–82.
51. Brown, M. F., and J. Seelig. 1978. Influence of cholesterol on the polar region of phosphatidylcholine and phosphatidylethanolamine bilayers. *Biochemistry*. **17**: 381–384.
52. Roberts, M. F., A. G. Redfield, and U. Mohanty. 2009. Phospholipid reorientation at the lipid/water interface measured by high resolution <sup>31</sup>P field cycling NMR spectroscopy. *Biophys. J.* **97**: 132–141.
53. Silver, E. T., D. G. Scraba, and R. O. Ryan. 1990. Lipid transfer particle-induced transformation of human high density lipoprotein into apolipoprotein A-I-deficient low density particles. *J. Biol. Chem.* **265**: 22487–22492.
54. Lusa, S., M. Jauhainen, J. Metso, P. Somerharju, and C. Ehnholm. 1996. The mechanism of human plasma phospholipid transfer protein-induced enlargement of high-density lipoprotein particles: evidence for particle fusion. *Biochem. J.* **313**: 275–282.
55. Liang, H. Q., K. A. Rye, and P. J. Barter. 1996. Remodelling of reconstituted high density lipoproteins by lecithin: cholesterol acyltransferase. *J. Lipid Res.* **37**: 1962–1970.
56. Rye, K. A., N. J. Hime, and P. J. Barter. 1997. Evidence that cholesteryl ester transfer protein-mediated reductions in reconstituted high density lipoprotein size involve particle fusion. *J. Biol. Chem.* **272**: 3953–3960.